

DESIGN OF A SLOTTED PATCH-BASED MULTIBAND ANTENNA WITH ENHANCED BANDWIDTH TO REDUCE CROSS-POLARIZED RADIATION

B. Bharani¹, N. E. V. Sai Kalyan², G. Vijay Chiranjeevi³, M. R. P. S. D. Polaraju⁴
^{1,2,3,4}Department of ECE, Vignan's Institute of Information Technology, Visakhapatnam, India.
Email: bavanabharani@gmail.com, ksai34190@gmail.com, vijaychiranjeevi28@gmail.com, r032788911@gmail.com

ABSTRACT:

This paper introduces a completely unique format of a compact and distinctly inexperienced tri-band antenna providing a single-patch configuration with five embedded ring slots and a Defected Ground Structure (DGS). The proposed rectangular patch antenna measuring 30mm x 30mm x 1.6mm is fabricated on an low-priced FR-4 substrate with the aid of using embedding ring slots withinside the patch the antenna is customized for wireless conversation systems including Wi-Fi (IEEE 802.11), WiMAX(IEEE 802.16) and 5G networks simulation research achieved using CST microwave studio software program elucidate the antennas traits the proposed format achieves splendid cross returned loss values of 34.4dB, 35.1 dB and 22 dB at frequencies of 3.046 GHz, 7.16 GHz, and 10.7 GHz respectively. Moreover, the antenna demonstrates income of 2.5 dBi, 2dBi and 3.2 dBi collectively with a directivity of 3.2 dBi. Incorporating the DGS slot enhances the antenna's overall performance, resulting in a couple of bands. This contemporary approach ensures progressed versatility and overall performance in wireless conversation applications.

INTRODUCTION:

The generation of unwanted radiation (also known as cross-polarization) from antennas is a major undertaking that negatively affects the structure of speech. Crosstalk caused by this phenomenon poses a serious threat to device performance. The main cause of cross-polarization generation is the development of higher-order orthogonal resonances that generate E-site additives orthogonal to the E-plane. These higher-order orthogonal modes are typically concentrated near the non-radiating edges of the patch, exacerbating the problem.

Various methodologies were explored withinside the literature to cope with this concern. For instance, strategies which includes the usage of shorting plates on the non-radiating edges were proposed [1]. Efforts directed in the direction of mitigating the effect of higher-order orthogonal modes and assuaging cross-polarization results constitute a pivotal approach in improving the general performance and reliability of conversation systems. One terrific approach, as elucidated withinside the literature, entails the usage of faulty patches coupled with shorting pins [2]. This method pursuits to cope with the have an effect on of higher-order orthogonal modes through strategically incorporating shorting pins at the side of defected patches. By doing so, the undesired results of cross-polarization may be efficaciously minimized, thereby contributing to the optimization of conversation gadget overall performance and reliability [2].

Defected Ground Structures (DGS) function pivotal additives in antenna design, presenting a flexible array of benefits at some point of several verbal exchange systems. By introducing styles or slots withinside the floor aircraft beneath the antenna structure, DGS complements antenna fashionable standard overall performance in numerous key aspects. These embody broadening antenna bandwidth, reducing cross-polarization effects, shaping radiation styles, suppressing floor waves, mitigating mutual coupling among antennas in array configurations, and facilitating antenna miniaturization. With their capability to tailor electromagnetic properties, DGS performs an essential characteristic in optimizing antenna efficiency, bandwidth, and easy machine reliability, making them critical factors in contemporary-day antenna engineering.

Various strategies related to Defected Ground Structures (DGS) have been explored to decorate the overall universal overall performance of smooth patch antennas, every imparting high-quality advantages. For instance, one method makes use of elliptical DGS to advantage a single-band reaction at the same time as simultaneously lowering cross-polarization stages with the beneficial useful resource of the usage of 16–18 dB [9]. Another method includes etching a notch at the threshold of the floor aircraft, which efficiently mitigates cross-polarization consequences. Additionally, the loading of an array of slots on the left floor aircraft has been installed to decorate antenna common universal overall performance. Moreover, the implementation of inverted U-formed strips on the pinnacle of the substrate has been determined to limiting unbalanced horizontal currents, thereby lowering cross-polarization with the beneficial useful resource of the usage of as a lousy lot as 19 dB [6]. These modern strategies underscore the persistent endeavors to refine antenna configuration and alleviate cross-polarization consequences making use of cutting-edge DGS methodologies. For example, the mixture of a Z-formed slot withinside the floor aircraft of a square patch antenna yields faded cross-polarization withinside the H-aircraft, showcasing a discount of about 22 dB withinside the operational bandwidth of 2.38–2.58 GHz [5].

Comparably, it has been found that the addition of three rectangular holes etched into the ground plane facilitates the coupling of weak fields, which in turn reduces cross-polarized radiation by 10 to 20 dB and mitigates leakage currents [12]. Furthermore, it is discovered that the efficient elimination of higher-order orthogonal modes results in a significant drop in cross-polarization, as low as -27.49 dB, when L-shaped DGS loading is integrated in a circularly polarized microstrip patch [3]. These examples are just a small portion of the creative approaches that have been described in the literature with the common goal of enhancing antenna performance and reducing cross-polarization effects.

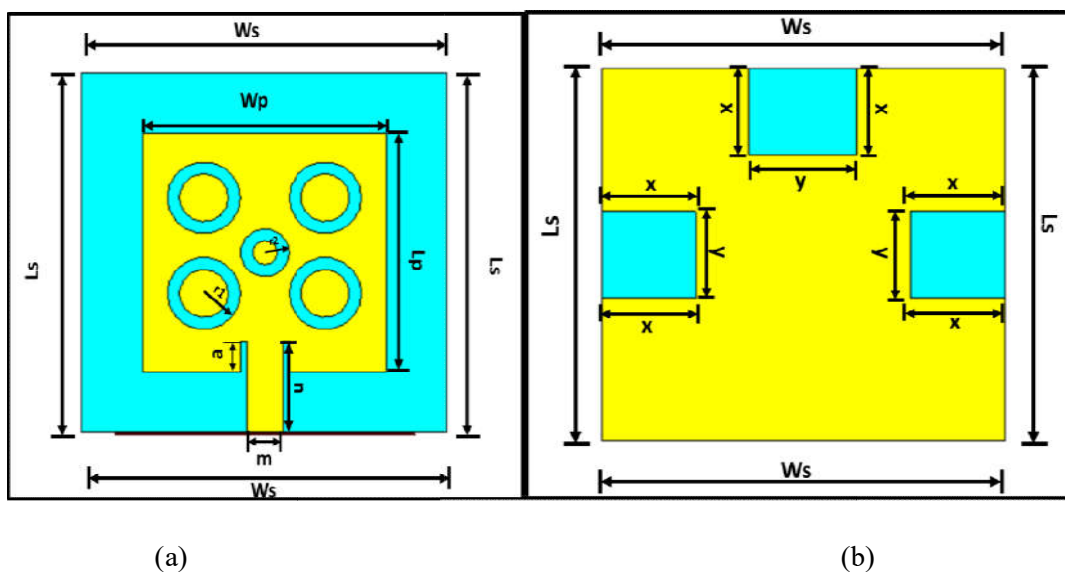


Figure 1: Proposed Antenna (a) Top View (b) Bottom View

In the contemporary-day investigation a centrally-fed round slotted patch complemented with the useful beneficial aid of the use of a couple of flawed ground configurations (FGCs) included into the substrate, has been advanced to create a triple-frequency antenna boasting decreased cross-polarized radiation within the course of every resonating band. Over the entire layout procedure each step has been exhaustively simulated the use of CST studio software ensuing within the success of a triple-frequency reaction characterized with the useful beneficial aid of the use of diminished cross-polarized radiation. Moreover, within the very last phase the advocated antenna famous indicates amplified gain better pondered photo coefficient and favorable radiation patterns various layout parameters of the proposed antenna were very well optimized via parametric evaluation to provide improvements in antenna performance. The authenticity of the simulated effects of the proposed layout has been showed via an assessment with the dimensions effects obtained from the fabricated prototype. The very last configuration of the proposed antenna is visually depicted in figure 1.

The article discusses the application of several techniques aimed at enhancing the performance of a conventional microstrip patch antenna. These techniques include the incorporation of slots and Defected Ground Structures (DGS) in the patch and ground plane, respectively, intending to achieve multi-resonance behavior while minimizing cross-polarization across all resonance bands. The proposed antenna design prioritizes simplicity and compactness, eschewing complex feeding mechanisms and intricate fabrication processes while eliminating back radiation. Notably, the antenna demonstrates reduced cross-polarized radiation across all resonance bands, a feature distinct from many existing designs in the literature, which typically focus solely on reducing cross-polar radiation at a single resonating band.

DESIGN PRINCIPLE:

The antenna configuration entails a square patch featuring ring-shaped apertures, accompanied by a ground plane exhibiting multiple anomalies, as illustrated in Figure 1. A circular ring-loaded patch, characterized by design parameters denoted as W_p and L_p , is affixed onto an FR4 epoxy substrate, with dimensional attributes denoted as W_s and L_s , as depicted in Figure 1. The dielectric constant and loss tangent of the substrate are specified as 4.3 and 0.02, respectively. A feedline, constructed with appropriate specifications denoted as m and n , is linked via a feeding aperture of radius 4 mm to achieve 50 Ohm impedance matching. The circular aperture, characterized by radii denoted as m and n , respectively, with a thickness denoted as t , is depicted in Figure 1(a). The formulas which are used to design the patch with desired values are shown below

$$\text{Width} = \frac{c}{2f_0 \sqrt{\frac{\epsilon_R + 1}{2}}}; \quad \epsilon_{eff} = \frac{\epsilon_R + 1}{2} + \frac{\epsilon_R - 1}{2} \left[\frac{1}{\sqrt{\left(1 + 12 \frac{h}{W}\right)}} \right]$$

$$\text{Length} = \frac{c}{2f_0 \sqrt{\epsilon_{eff}}} - 0.824h \left[\frac{(\epsilon_{eff} + 0.3) \left(\frac{W}{h} + 0.264\right)}{(\epsilon_{eff} - 0.258) \left(\frac{W}{h} + 0.8\right)} \right]$$

Table 1. Design specifications of the proposed antenna.

Parameters	Values(mm)	Parameters	Values(mm)	Parameters	Values(mm)
W_s	30	m	3	y	8
L_s	30	n	7.6	r_1	4
W_p	20	Copper height	0.035	r_2	3
L_p	20	Substrate-Height	1.6	-	-
a	2.6	x	7	-	-

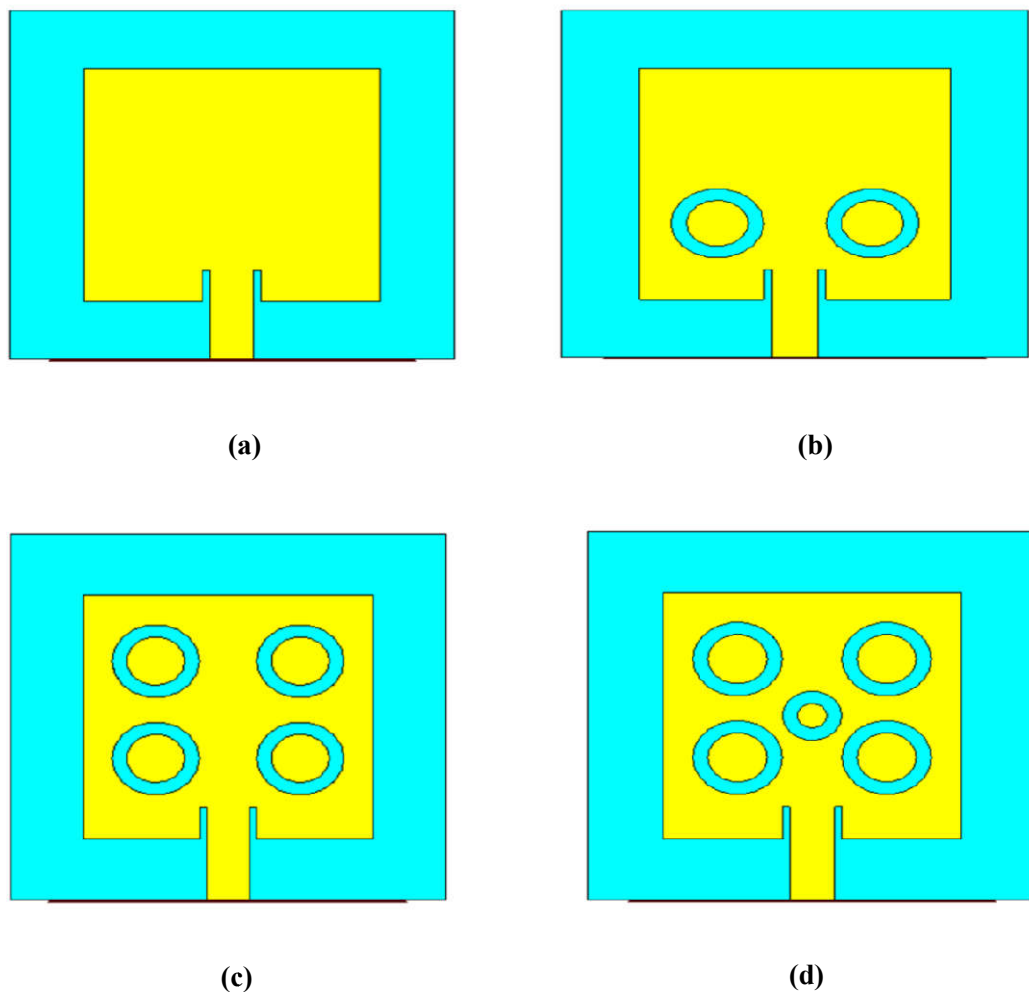


Figure 2. Design stages. (a) Stage-1. (b) Stage-2. (c) Stage-3. (d) Stage-4.

Initially, it became determined to not forget an inset-fed square-shaped patch to make certain impedance matching. In this approach, a small slot was created on the decrease fringe of the patch, called the feeding slot. Subsequently, the feedline became linked to the patch via the feeding slot, as illustrated in Figure 2(a). In the inset feeding mechanism, exquisite emphasis became located on figuring out the appropriate region of the feeding point. Parametric evaluation became performed to examine the precise feeding region with the aid of using various the slot length (a). Since the conventional patch antenna is meant for single-band resonance, ring-shaped slots have been integrated into the patch, as depicted in Figure 2(b), to gather extra frequency bands. The incorporation of ring-shaped slots, all of same length and shape, onto the patch brought sizable disturbances within the E-discipline distribution below the patch, ensuing in a growth in present day alongside the brink and a lower in present day via the surface. This facilitated the attainment of extra frequency bands with brought advantage for the designed antenna. A ring-shaped slotted patch yielded one extra resonance within the better frequency range. To reap better resonance frequencies in different bands, ring-shaped slots have been supplemented with a smaller ring-shaped slot within the middle of the patch, as proven in Figure 2(c) and Figure 2(d).

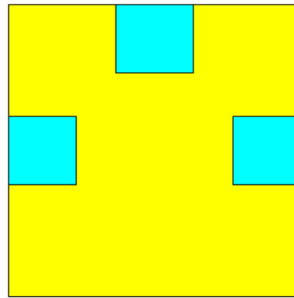


Figure: 3(a)

To broaden the frequency bands in the targeted lower frequency range, modifications were made to the ground plane by integrating a slit at the base of the substrate, as shown in Fig. 1(b). The appearance of defective ground structures (DGS) caused significant disturbances in the E field around the ground plane, leading to increased E field distribution at the periphery of the slots and at the upper end of the ground plane, as shown in Figure 1(b). At the same time, a decrease in the electric field is observed in the lower part of the ground plane. Therefore, DGS has created multiple current pathways, leading to multi-band resonance. Although a slotted patch with a single DGS produced a multiband response, multiple bands were observed to have high reflectivity. To solve this problem, three additional DGS were integrated on each slope of the ground plane except the bottom edge, as shown in Fig. 2(d). This effect balances the strong components of the electric field in the opposite direction, leading to an improvement in the reflection coefficient. The size of the slots in the ground plane was optimized by parametric analysis.

REDUCTION IN CROSS-POLARIZED RADIATION:

The reduction of cross-polarized radiation is an essential aspect of antenna system design and optimization, especially in situations where sign integrity and overall spectral standard performance are critical. Cross-polarized radiation, which happens when electromagnetic waves oscillate in planes orthogonal to the known polarization, can result in sign degradation, interference, and reduced overall system performance. Addressing this issue requires a detailed understanding of the underlying concepts that govern antenna conduct and radiation patterns. Surface cutting-edge radiation styles provide vital insights into the distribution of electromagnetic electricity and serve as a foundation for developing methods to lessen cross-polarized radiation. This study looks into the usage of cutting-edge radiation types as a strategy for reducing cross-polarized radiation, resulting in a completely novel technique for improving antenna.

The major supply of cross-polarized radiation, that is typically located close to the non-radiating edges of an object, is the orthogonal E-discipline additives similar to better-order resonance modes [20]. Figure 4 (a) indicates the E-discipline distribution within the patch without time intervals. It may be located that there are orthogonal modes close to the non-radiating edges of the patch. Figure 4(b) illustrates the terrestrial E-discipline distribution without DGS. It must be mentioned that maximum of the E-discipline additives is focused within the decrease a part of the earth, ensuing in a better leakage modern and accelerated cross-polarized radiation. In this study, the outcomes of the illness floor shape and grooved web website online applied within the layout at the cross-polarization attenuation in each the E and H planes are studied. Significant interference within the fields take place beneath Neath the place due to the fact the voids extrude the radiation conduct of the designed antenna. This consequences in a discount of the orthogonal E-discipline additives close to the non-radiating area, canceling the better-order modes, as proven in Fig. 4(c). At the equal time, the E-discipline additives of the emitting area chargeable for co-polarization continue to be unchanged. A square slot at the floor and 3 same square slots at the rims of the bottom plate lessen cross-polarized radiation. The DGS impact on the area, collectively with the substrate floor, extensively perturbs the sector, for that reason minimizing the sector additives at the lowest and suppressing the robust leakage modern.

Consequently, this consequences in a lower in cross-polarized radiation. Additionally, the slot withinside the floor is applied to neutralize a part of the sector additives outflowing from the patch, main to a lower in cross-polarized radiation. The E-discipline distributions alongside the floor aircraft with the DGS impact are illustrated.

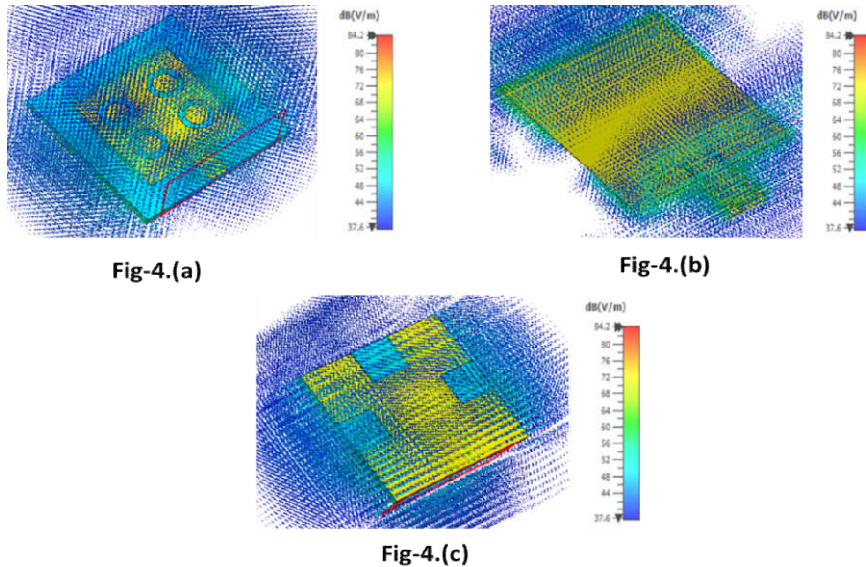


Figure4.E-fielddistribution.(a)Patchwithslots.(b) Patch without slots(c)Ground with DFG

RESULTS AND DISCUSSIONS:

ReflectionCoefficientandBandwidth:

Evaluating the mirrored image coefficient and bandwidth of the designed antenna at distinct degrees indicates that innovative enhancements have been executed via way of means of incorporating state-of-the-art layout elements. In segment 1, the usage of DefectedGroundStructure (DGS) in parallel with easy patches yields promising results. At 3.01 GHz, the antenna reveals an extensive return loss of -21 dB, indicating impedance matching and minimum contemplated power. With a bandwidth of 400MHz, this antenna gives versatility over an extensive frequency range return loss is barely decreased. At 7.3GHz and 10.6 GHz, even as keeping an extensive stage of impedance matching at 150MHz and 200MHz bandwidths respectively, taking into account targeted resonant capability even as keeping operational flexibility is shown.

Proceeding to Stage-2, integration of the DFG with two ring-shaped slotted patches yields impressive results. At 3.04 GHz, the antenna achieves an outstanding return loss of -36.7 dB, denoting excellent impedance matching. The accompanying bandwidth of 350 MHz underscores its adaptability across various communication scenarios. At higher frequencies, the return losses remain commendable, maintaining efficient impedance matching, albeit with narrower bandwidths, suggesting focused resonance capabilities suitable for specific frequency ranges.

Stage-3 introduces in addition refinements with the incorporation of 4 asymmetrically located ring-formed slotted patches along the DFG. Resonating frequencies at 3.1 GHz, 7.18 GHz, and 10.76 GHz showcase strong return losses and bandwidths, indicative of more suitable overall performance and flexibility throughout a much wider frequency spectrum in comparison to in advance stages.

Finally, Stage-4 showcases the culmination of improvements with the integration of five ring-shaped slotted patches alongside the DFG, yielding superior results compared to preceding stages. The achieved return losses at 3.046 GHz, 7.16 GHz, and 10.7 GHz, coupled with their respective bandwidths, signify enhanced impedance matching and operational flexibility, underscoring the effectiveness of the proposed antenna design. The proposed antenna surpasses previous stages in terms of return losses and bandwidths, highlighting its efficacy in achieving robust impedance matching and minimizing reflected power across diverse frequency ranges. This iterative refinement process demonstrates the progressive optimization of antenna performance, making it a compelling choice for a wide array of communication applications requiring reliable and efficient operation across multiple frequency bands.

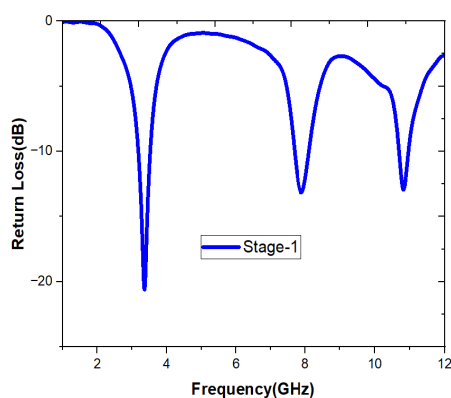


Fig: 5(a)

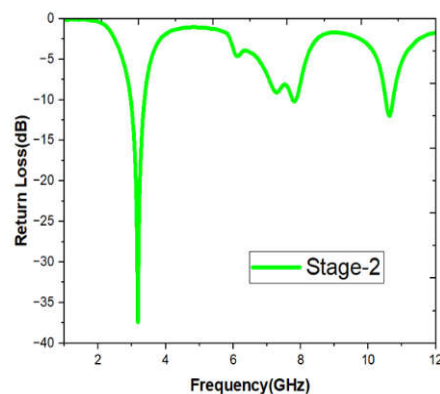


Fig: 5(b)

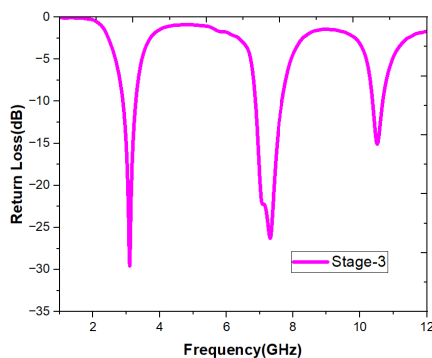


Fig: 5(c)

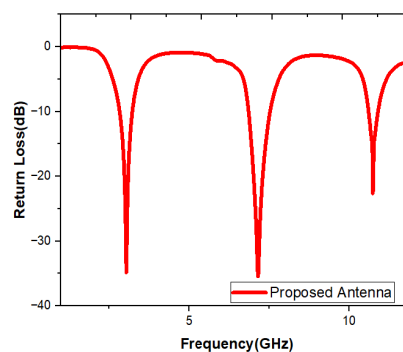


Fig: 5(d)

Figure 5. Reflection coefficient variation in Stage-1 (a), Stage-2 (b), Stage-3 (c) and Proposed Antenna (d).

Table 2. Resonance characteristics of all design stages of the proposed antenna.

Stages	Resonant frequency (GHz)	Reflection coefficients (dB)	Bandwidth (MHz)
Stage-1	3.01,7.3,10.6	-21,-14,-13.6	400,150,120
Stage-2	3.04,7.1,10.7	-36.7,-12,-13.5	350,200,150
Stage-3	3.1,7.18,10.76	-30.8,-27.3,-17.6	330,600,300
Proposed antenna (Simulated)	3.046,7.16,10.7	-34.4,-35.1,-22	400,750,450

Co-polarization and Cross-polarization patterns in E-plane and H-plane.

The designed antenna showcases extraordinary overall performance attributes regarding each co-polarization and cross-polarization throughout a spectrum of frequencies. In the electrical plane (E-plane), mainly at frequencies spanning 3.046 GHz, 7.16 GHz, and 10.7 GHz, the antenna well-known shows strong co-polarization characteristics, putting forward its adeptness in successfully transmitting and receiving alerts exactly aligned with its unique polarization axis. Conversely, inside the magnetic plane (H-plane), it manifests a commendable potential for attenuating cross-polarization, efficaciously mitigating the transmission and reception of alerts orthogonal to the supposed polarization route throughout the equal frequency variety. This holistic overall performance profile underscores the antenna’s applicability in situations necessitating reliable and particular sign propagation and reception throughout a numerous variety of frequency allocations.

Figure 6. Stage-1 simulated patterns of E-plane Co-polarization, and Cross-polarization at (a) 3.01GHz (b) 7.3GHz (c) 10.6GHz

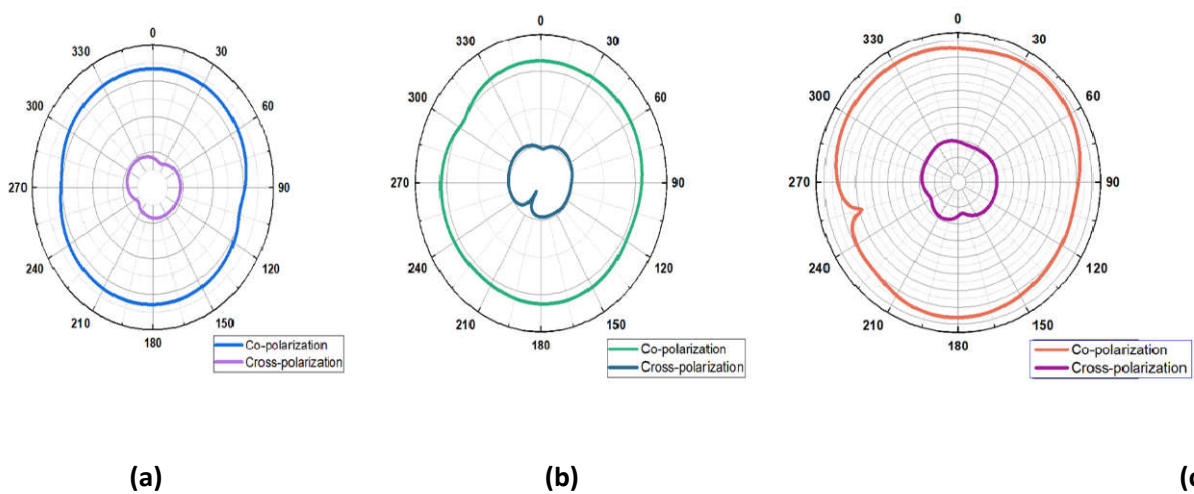


Figure7.Stage-1 simulated patterns of H-plane Co-polarization, and Cross-polarization at (a)3.04GHz (b)7.3GHz (c)10.6GHz

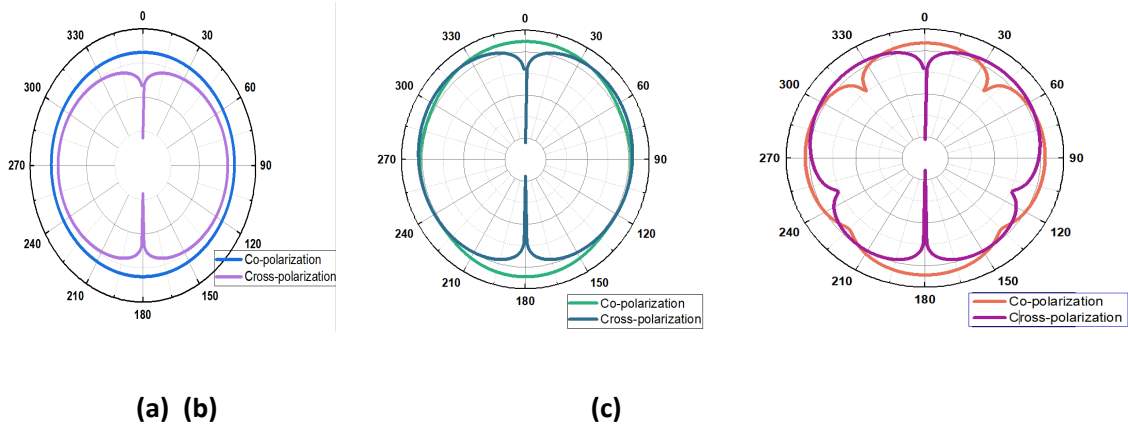


Figure8.Stage-2 simulated patterns of E-plane Co-polarization, and Cross-polarization at (a)3.04GHz (b)7.1GHz (c)10.7GHz

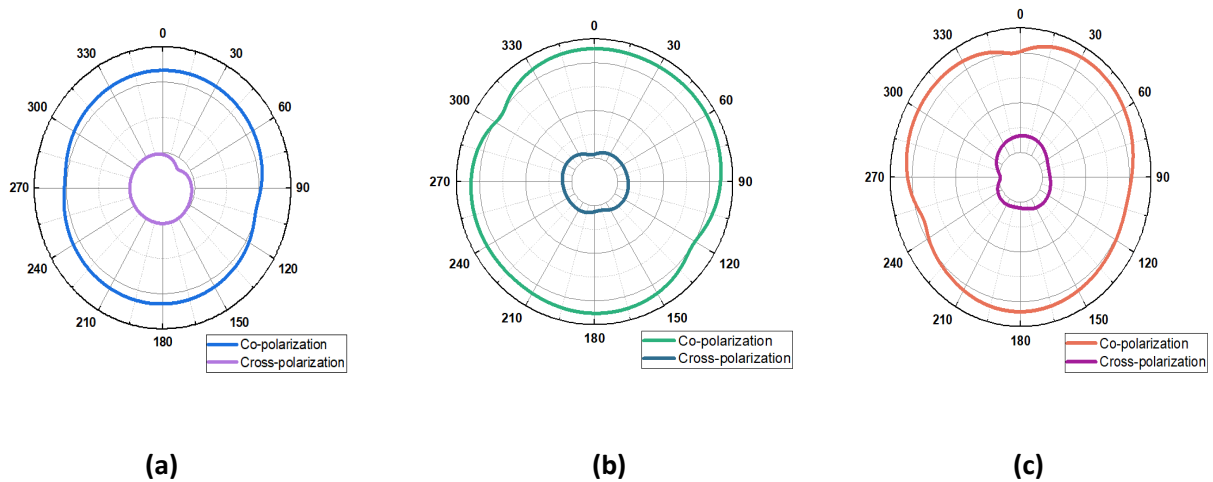


Figure9.Stage-2 simulated patterns of H-plane Co-polarization, and Cross-polarization at (a)3.04GHz (b)7.1GHz (c)10.7GHz

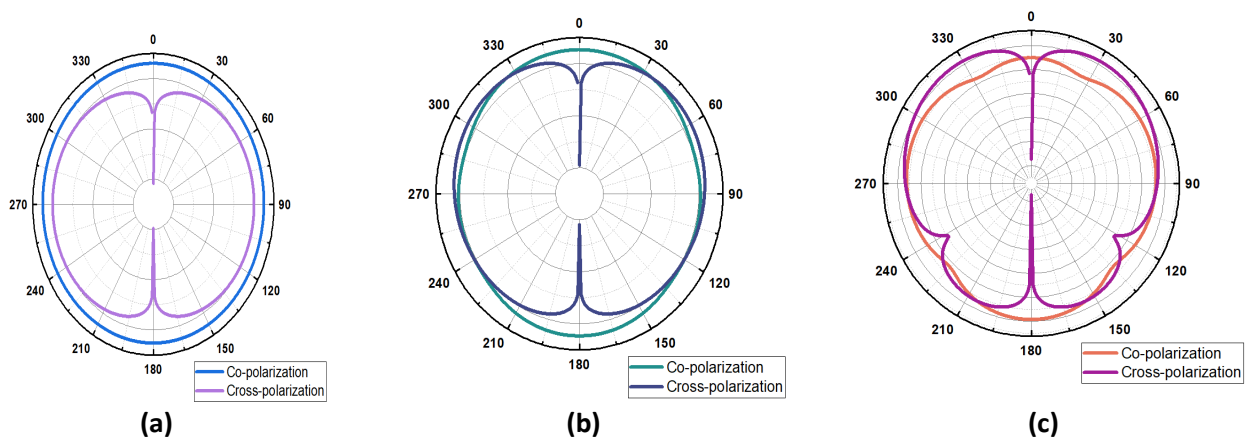
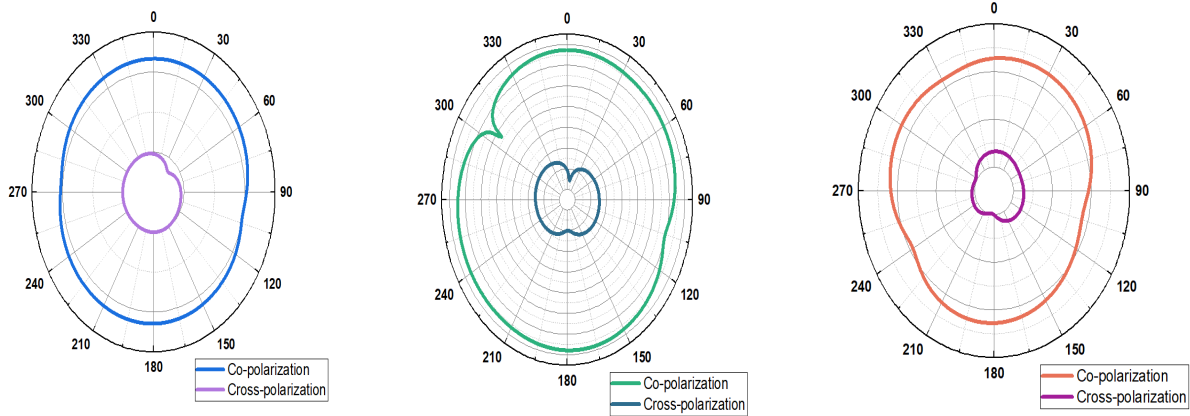
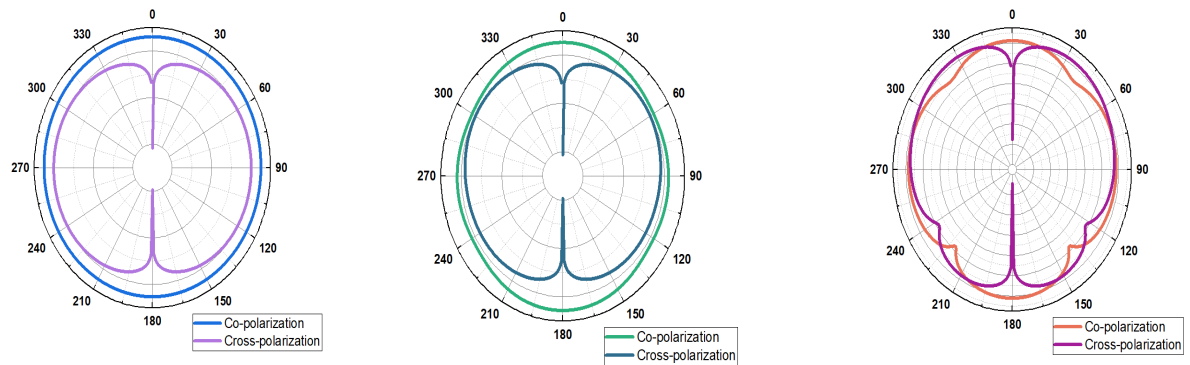


Figure10. Stage-3 simulated patterns of E-plane Co-polarization, and Cross-polarization at (a) 3.1GHz (b) 7.18GHz (c) 10.76GHz



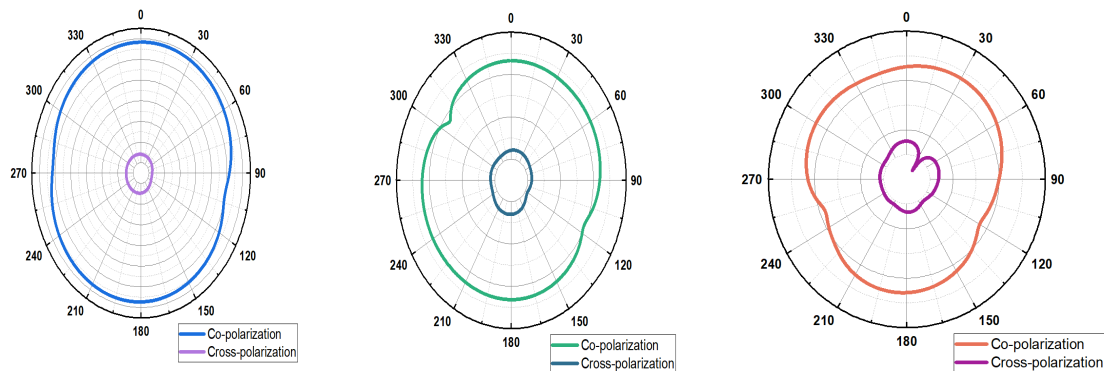
(a) (b) (c)

Figure11. Stage-3 simulated patterns of H-plane Co-polarization, and Cross-polarization at (a) 3.1GHz (b) 7.18GHz (c) 10.76GHz



(a)(b) (c)

Figure12. Proposed Antenna simulated patterns of E-plane Co-polarization, and Cross-polarization at (a) 3.046GHz (b) 7.16GHz (c) 10.7GHz



(a) (b) (c)

Figure13.Proposed Antenna simulated patterns of H-plane Co-polarization, and Cross-polarization at (a)3.04GHz (b)7.4GHz (c)10.7GHz

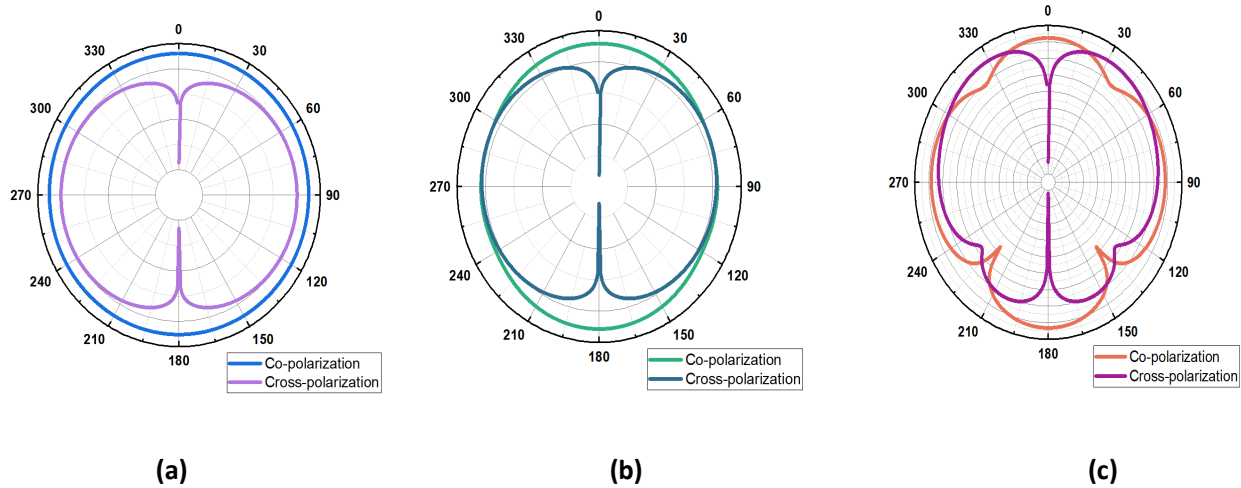


Table3.Proposed Antenna E-plane co-and cross-polarization of the proposed antenna at principal radiating direction.

Resonant Frequency (GHz)	Simulated Co-pol gain (dB)	Simulated Cross-pol gain (dB)
3.046	2.565	-20
7.16	2.6	-26.42
10.7	2.07	-32

Table4.Proposed Antenna H-plane co-and cross-polarization of the proposed antenna at principal radiating direction.

Resonant frequency (GHz)	Simulated Copol gain (dB)	Simulated Crosspol gain (dB)
3.046	2.537	-30.7
7.16	2.87	-26.8
10.7	2	-29.98

Radiation Efficiency and Gain

The completed radiation efficiencies right here on the targeted frequencies imply how properly the antenna converts a good-sized percent of the provided energy into electromagnetic radiation. The antenna obtains a benefit of 2.565dB and a remarkable radiation performance of 74% at 3.046 GHz, suggesting extraordinarily green use of enter energy for radiation purposes. At better frequencies of 7.16 GHz and 10.7 GHz, the radiation efficiencies are nonetheless good sized no matter a minor reduction; they sign up values of 60.6% and 59.74%, respectively, and the benefit at those frequencies is 2.6 dB and 2.07 dB respectively.

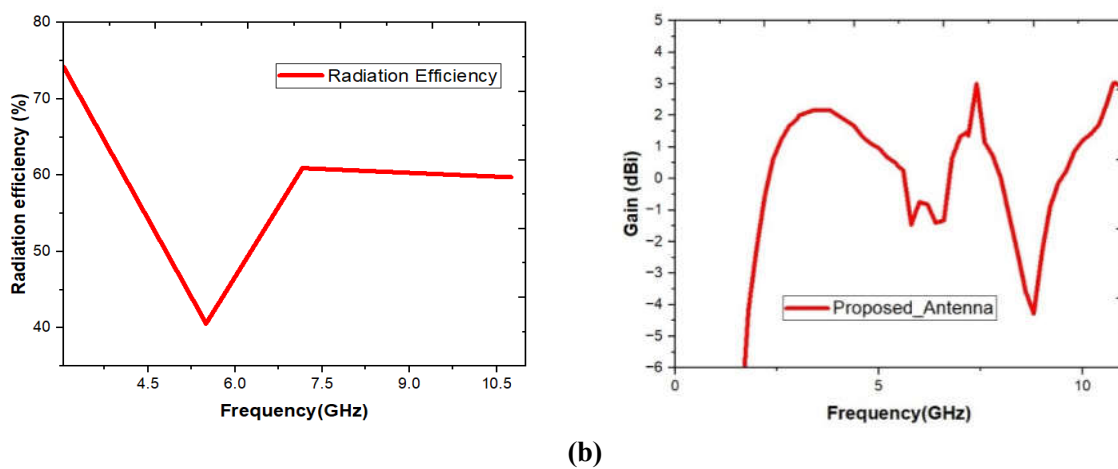


Fig:14(a) Radiation Efficiency and **(b)** Gain of the proposed antenna

Table5.The radiation efficiency of the proposed antenna.

Resonant frequency (GHz)	Simulated gain (dB)	Simulated Efficiency (%)
3.046	2.565	74.23
7.16	2.6	60.67
10.7	2.07	59.74

Table 6. Comparison of the designed antenna with different existing works.

References	Antenna size (mm ²)	Nature	Cross-pol reduction technique	Cross-pol reduction level (dB)
[3]	59.5×64.5	Singleband	L-shaped DGS	-27.49
[4]	68×68	Singleband	Slots in ground	-20
[5]	38×47	Singleband	Z-shaped DGS	-22
[6]	50×60	Singleband	Array of slots	-19.08
[8]	31×31	Dual-band	Vias, stubs, metallic shield	-25
[10]	80×74.2	Singleband	Spiral SRR	-12
[11]	70×70	Singleband	Anisotropic substrate	-28
[12]	125×200	Dual-band	Array of shorting pins	-23.5
[13]	53.47×44.05	Singleband	DPS with shorting pin	-30
Proposed design	30×30	Tri-band	Defected patch with multiple DGS	-32

CONCLUSION:

In conclusion, the end result of meticulous layout concerns and rigorous trying out has resulted within the improvement of an antenna device that epitomizes efficiency, versatility, and overall performance excellence. Through iterative refinement and optimization throughout a couple of stages, the proposed antenna has validated top notch talents in phrases of impedance matching, radiation efficiency, and cross-polarization suppression throughout a numerous variety of frequencies.

The usage of superior layout factors consisting of Defected Ground Structure (DGS) and strategically placed slotted patches has established instrumental in improving the antenna's resonance traits and minimizing undesirable radiation patterns. The done effects underscore the antenna's adaptability to diverse communicate scenarios, presenting dependable sign transmission and reception throughout specific frequency bands.

Moreover, the found radiation efficiencies, coupled with the amazing go back loss values and bandwidths, validate the antenna's efficacy in successfully changing enter electricity into radiated electromagnetic strength whilst retaining strong impedance matching.

In essence, the proposed antenna represents an end result of innovation, precision engineering, and thorough analysis, positioning it as an impressive contender within the realm of contemporary-day communicate systems. Its capacity to supply constant and high-overall performance operation throughout numerous frequency degrees makes it a compelling desire for a big range of applications, from wi-fi communicate networks to satellite tv for pc communicate systems. With its first-rate overall performance metrics and flexible layout, the proposed antenna stands as a testimony to the ability of superior antenna engineering in shaping the destiny of wi-fi communicate technology.

REFERENCES

1. Poddar, R., S. Chakraborty, and S. Chattopadhyay, "Improved cross polarization and broad impedance bandwidth from simple single element shorted rectangular microstrip patch: theory and experiment," *Frequenz*, Vol. 70, No. 1-2, 1-9, DOI 10.1515/freq-2015-0105, 2016.
2. Ghosh, A., S. Chattopadhyay, L. L. K. Singh, et al., "Wide bandwidth microstrip antenna with defected patch surface for low cross polarization applications," *Int JRF Microw Comput Aided Eng.*, e21127, <https://doi.org/10.1002/mmce.21127>, 2017.
3. Anita, R. and M. V. Kumar, "Cross polarization reduction of a circular polarized microstrip antenna with two L slot DGS for wireless applications," *International Journal of Pure and Applied Mathematics*,

- Vol. 120, No. 6, 1173–1188, 2018.
4. Liu, N., S. Gao, L. Zhu, et al., “Low-profile microstrip patch antenna with simultaneously enhanced bandwidth, beamwidth, and cross-polarization under dual resonance,” *IET Microw. Antennas Propag.*, Vol. 14, No. 5, 360–365, The Institution of Engineering and Technology, 2020.
 5. Acharjee, J., A. K. Singh, K. Mandal, et al., 2019, “Defected ground structure toward cross polarization reduction of microstrip patch antenna with improved impedance matching,” *Radio Engineering*, Vol. 28, No. 1, DOI: 10.13164/re.2019.0033, April 2019.
 6. Wang, C. J., “Methods of suppression of cross-polarized power for the CPW-fed monopole antenna,” *Microw Opt Technol. Lett.*, Vol. 59, 1968–1975, <https://doi.org/10.1002/mop.30657>, 2017.
 7. Huang, H., X. Zhang, S. Xie, W. Wu, and N. Yuan, “Suppression of cross-polarization of the microstrip integrated balun-fed printed dipole antenna,” *Hindawi Publishing Corporation International Journal of Antennas and Propagation*, Vol. 2014, 8 pages, Article ID 765891, <http://dx.doi.org/10.1155/2014/765891>, 2014.
 8. Meng, C., J. Shi, and J. Chen, “Flat-gain dual-patch antenna with multi-radiation nulls and low cross-polarization,” *Electronics Letters*, Vol. 54, No. 3, 114–116, 2018.
 9. Heydari, R. D. and N. Moghadasi, “Introduction of a novel technique for the reduction of cross polarization of rectangular microstrip patch antenna with elliptical DGS,” *Journal of Electromagnetic Waves and Applications*, Vol. 22, No. 8–9, 1214–1222, DOI: 10.1163/156939308784158788, 2008.
 10. Ghosh, C. K., B. Rana, and S. K. Parui, “Reduction of cross-polarization of slotted microstrip antenna array using spiral-ring resonator,” *Microwave and Optical Technology Letters*, Vol. 55, No. 9, DOI 10.1002/mop, 2013.
 11. Shi, H., S. Zhu, J. Li, et al., “Cross-polarization suppression in C-shaped microstrip patch antenna employing anisotropic dielectrics,” *Journal Of Advanced Dielectrics*, Vol. 7(4), 1750026 (5 pages), DOI: 10.1142/S2010135X17500266, 2017.
 12. Khouser, H. and Y. K. Choukiker, “Cross polarization reduction using DGS in microstrip patch antenna,” *International conference on Microelectronic Devices, Circuits and Systems (ICMDCS)*, 10–12, August 2017, Vellore, India, DOI: 10.1109/ICMDCS.2017.8211577, 2017.
 13. Singh, A., S. Vijay, and R. N. Baral, “Low cross-polarization improved-gain rectangular patch antenna,” *Electronics*, Vol. 8, 1189, doi: 10.3390/electronics8101189, www.mdpi.com/journal/electronics, 2019.
 14. Dash, R. K., P. B. Saha, and D. Ghoshal, “Design of a equally spaced U-shaped slotted patch antenna with defected ground structure for multiband applications,” *7th International Conference on Signal Processing and Integrated Networks (SPIN)*, Noida, India, DOI: 10.1109/SPIN48934.2020.9071199, February 27–28, 2020.
 15. Badr, S. and K. I. Ehab, “Design of multiband microstrip patch antenna for WiMax, C-band and X-band applications,” *Aswan Engineering Journal (AswEJ)*, <https://www.researchgate.net/publication/324597715>, 2018.
 16. Kaushal, D. and T. Shanmuganatham, “A Vinayak slotted rectangular microstrip patch antenna design for C-band applications,” *Microw. Opt. Technol. Lett.*, Vol. 59, 1833–1837, <https://doi.org/10.1002/mop.30628>, 2017.

17. Roy, B., A. Bhattacharya, S. Mondal, et al., "Size miniaturization of microstrip antenna embedded with open-ended grounded slots," *J. Comput. Electron.*, DOI 10.1007/s10825-017-0995-6, 2017.
18. Hajlaoui, A. E., "New triple band electromagnetic band gap microstrip patch antenna with two shaped parasitic elements," *J. Comput. Electron.*, DOI 10.1007/s10825-017-1100-x, 2017.
19. Ali, T., K. D. Prasad, and R. C. Biradar, "A miniaturized slotted multiband antenna for wireless applications," *Journal of Computational Electronics*, <https://doi.org/10.1007/s10825-018-1183-z>, 2018.
20. Dash, R.K., P.B.Saha, D.Ghoshal, and G.Palai, "Design of triangular shaped slotted patch antennas for both wideband and multiband applications," *International Journal of Applied Electromagnetics and Mechanics*, Vol. 68, No. 3, 275–294, 2022.